NMR Studies of Electrostatic Potential Distribution around Biologically Important Molecules

Gertz I. Likhtenshtein,* Itay Adin,* Artem Novoselsky,* Alexander Shames,# Iris Vaisbuch,* and Robert Glaser*
Departments of *Chemistry and #Physics, Ben-Gurion University of the Negev, Beer-Sheva 84105, Israel

ABSTRACT A new experimental approach has been developed to study the distribution of local electrostatic potential around specific protons in biologically important molecules. The approach is the development of a method denoted as "spin label/spin probe," which was proposed by one of us (Likhtenshtein et al., 1972. *Mol. Biol.* 6:498–507). The proposed method is based upon the quantitative measurement of the contribution of differently charged nitroxide probes to the spin lattice relaxation rate ($1/T_1$) of protons in the molecule of interest, followed by calculation of local electrostatic potential using the classical Debye equation. In parallel, the theoretical calculation of potential distribution with the use of the MacSpartan Plus 1.0 program has been performed. Application of the method to solutions of simple organic molecules (aliphatic and aromatic alcohols, aliphatic carboxylates (propionate anion), and protonated ethyl amine and imidazole) allowed us to estimate the effective potential around the molecules under investigation. These were found to be in good agreement with theoretically expected values. This technique was then applied to zwitterionic amino acids bearing neutral and charged side chains (glycine, lysine, histidine, and aspartic acid). The reliability of the general approach is proved by the data presented in this paper. Application of this new methodology can afford insight into the biochemical significance of electrostatic effects in biological systems.

INTRODUCTION

Electrostatic interactions play a key role in the structure and function of biological molecules. Association of proteins in solution and in membranes, protein-nucleic acid and nucleic acid-nucleic acid interactions, enzyme-substrate complexation, chemical reactions in enzyme active sites, charge transfer, voltage gating of membrane channels, folding and unfolding processes of biopolymers, etc. are all drastically affected by the strength and distribution of the electrostatic field around various regions in biological molecules.

At one time or another, much of the wide methodological and theoretical arsenal of chemical physics has been used to study electrostatic interactions in biological and chemical systems. Significant progress has been achieved in the theoretical calculation of these interactions. The most advanced theoretical approach to the problem relies upon the use the Poisson-Debye equation for polarizable solutes of known structure embedded in a dielectric medium (e.g., Klapper et al., 1986; Gilson and Honig, 1988; Gilson et al., 1987; Sharp and Honig, 1990; Bashford and Karplus, 1990; Bajorath et al., 1991 Beroza et al., 1991; Aqvist et al., 1991; Tidor and Karplus, 1991; Sharp et al., 1992; Bashford and Gerwert, 1992; Honig et al., 1993; Gilson, 1993; Yang et al., 1993; Scott et al., 1994; Anni et al., 1994; Honig and Nicholls, 1995). In the accepted model, one supposes the existence of two dielectric continuums: one of low dielectric constant (ϵ) for solutes and one of high ϵ ($= 80$) for the surrounding bulk aqueous phase.

Two types of experimental methods for the investigation of local electrostatic fields in the vicinity of definite (specific) parts of biological molecules were proposed. The first group of methods is based upon electrostatic measurements utilizing static local parameters, such as the pK of a chosen protein or polypeptide functional group or the spectral characteristics of a chromophore attached to a biopolymer, i.e., the Stark effect (see, for example, Sitkoff et al., 1994, and references therein). While the results obtained by these various methods are in good agreement with the theoretically predicted values, in most cases it is necessary to bear in mind that experimentally determined pK and Stark effect parameters may be effected by factors other than local electrostatic fields (such as local donor-acceptor interactions, local dielectric constants, steric accessibility to solvent, etc.). The physical basis of the second type of approach rests upon the effect of the local electrostatic potential upon dynamic interactions at encounters with charged quenching molecules, resulting in fluorescence (phosphorescence) (Druzhinin et al., 1986; Anni et al., 1994), or between a stable radical (e.g., nitroxide) and another charged paramagnetic species (Likhtenshtein et al., 1972; Likhtenshtein, 1976, 1988, 1993). In such cases, the relaxation parameters, i.e., the lifetime of the fluorescence (phosphorescence) chromophore or spin-spin and spin-lattice relaxation rates of paramagnetic species are dependent upon the frequency of encounters, and, therefore, on local electrostatic fields (Tsui et al., 1990; Hecht et al., 1995).

Received for publication 17 August 1998 and in final form 12 February 1999.

Address reprint requests to Prof. Gertz I. Likhtenshtein or Prof. Robert Glaser, Department of Chemistry, Ben-Gurion University of the Negev, Beer-Sheva 84105, Israel. Tel.: 972-7-647-2189 ( ) or 972-7-646-1194 (R. G.); Fax: +972-7-647-2943 (attn. Likhtenshtein or Glaser); E-mail: gertz@bgumail.bgu.ac.il or glaser@bgumail.bgu.ac.il.

0006-3495/99/07/443/11 $2.00

In particular, it was established (Likhtenshtein et al., 1972; Likhtenshtein, 1976, 1988, 1993) that the spin exchange rate constants (k_{ex}) in solution between nitroxide radicals of different charges (**I-III**) and positive (diphenylchromium) or negative (ferricyanide) complexes are strongly dependent upon the following factors, which are in approximate agreement with the Debye theory: 1) the product of the charges (Z_1*Z_2), 2) the distance between the charges within the encounter complex, and 3) the ionic strength. It was also shown (Likhtenshtein et al., 1970, 1972; Likhtenshtein, 1976, 1988, 1993) that k_{ex} values depend upon steric factors in the vicinity of encounter particles, as well as upon the electronic structure (spin-spin relaxation parameters) of the paramagnetic complexes.

The effectiveness of nitroxides and paramagnetic metal complexes as relaxation reagents for protons has been widely demonstrated for both static and dynamic systems (Roberts et al., 1969; Taylor et al., 1969; Mildvan and Weiner, 1969; Reuben and Kayne, 1971; Dwek, 1972; Wien et al., 1972; Syrtzova et al., 1972, 1974; Krugh, 1971; Lezina et al., 1976; Likhtenshtein, 1976, 1993; Sletten et al., 1983; Niccolai et al., 1982; Navon and Valensin, 1987; Vold et al., 1968). In contrast to nitroxides, metal complexes and luminescence chromophores show a certain preferred affinity toward some functional groups, and therefore their use is limited. A general limitation of the last two methods is that they are applicable only to systems with pronounced luminescent or paramagnetic properties (Tsui et al., 1990; Hecht et al., 1995).

In this report we present an investigation of the distribution of the electrostatic potential around simple charged organic molecules and amino acids, utilizing both experimental and theoretical approaches. As part of this study, a new general approach was developed to study local potential distribution around specific protons in the vicinity of functional groups within biologically important molecules. This approach relies upon a quantitative measurement of the contribution of differently charged nitroxide probes to spin relaxation rates of various protons in the molecule of interest, followed by a calculation of local electrostatic charges, using the classical Debye equation. In parallel, the theoretical calculation of electrostatic potential distribution with the use of the MacSpartan Plus 1.0 program has been performed on the target molecules. Application of the method to solutions of simple organic molecules (aliphatic and aromatic alcohols, aliphatic carboxylates (propionate anion), and protonated ethyl amine, imidazole) allowed us to estimate effective potentials around the molecules under investigation. These were found to be in good agreement with theoretically expected values. This technique was then applied to zwitterionic amino acids bearing neutral and charged side chains (glycine, lysine, histidine, and aspartic acid). The reliability of the general approach is proved by the data presented in this paper. Application of this new methodology can afford insight into the biochemical significance of electrostatic effects in biological systems.

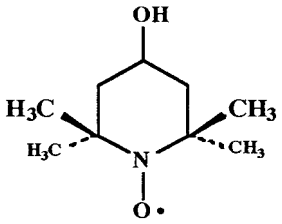

Scheme **I**.

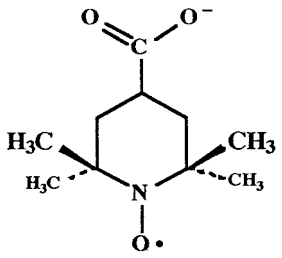

Scheme **II**.

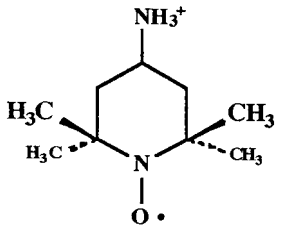

Scheme **III**.

MATERIALS AND METHODS

Materials

Spin probes 4-hydroxy-TEMPO (TEMPO-2,2,6,6-tetramethyl-l-piperidinyloxy free radical) (Scheme **I**), 4-amino-TEMPO (Scheme **III**), deuterium oxide (99%), aliphatic alcohols, benzyl alcohol, sodium propionate, ethylamine, imidazole, and amino acids were purchased from Sigma Chemical Co. TEMPO-4-carboxylic acid (Scheme **II**) was purchased from Aldrich Chemical Co.

Sample preparation

A solution containing 10 mM of the target molecule in D_2O was mixed with an appropriate amount of D_2O solution containing 10 mM of the target molecule and 6.0 mM nitroxide spin probe to afford final spin probe concentrations of 2.4, 3.6, 4.8, and 6.0 mM. Before mixing, the pD of each solution was adjusted with NaOD or DCl to ensure functional group ionization in the charged spin-probe (pD $\approx$ 7 for solutions containing negatively charged spin probe (Scheme **II**) and pD $\approx$ 4 for those having positively charged spin probe (Scheme **III**) (with the exception of propionate anion/spin probe (Scheme **III**) solutions, in which the pD was adjusted to $\sim$6.5)).

NMR measurements

^{1}H NMR spectra (5-mm sample tubes, 298 K) and the measurement of ^{1}H T_1 relaxation times were performed at 500.1 MHz on a Bruker DMX-500

Fourier transform spectrometer. The deuterated solvent was used as an internal lock, and the residual HOD solvent was used as an internal reference (δ_H 4.7). Standard Bruker microprograms were utilized for the fast inversion recovery technique (Vold et al., 1968; Freeman and Hill, 1969).

ESR measurements

Concentrations of nitroxide probes (Schemes **I–III**) in solutions used in the NMR T_1 experiments were measured by electron spin resonance (ESR) spectroscopy. Solutions were placed in 110-mm length, 1-mm i.d. glass capillary tubes centered in the rectangular cavity of the probe. Electron paramagnetic resonance (EPR) spectra were recorded using a Bruker EMX-220 digital X-band spectrometer equipped with a Bruker ER 4121VT temperature control system at 297 K. Spectra were obtained with the following parameters: 9.40 GHz microwave frequency; 2.012 mW nonsaturated microwave power; 100 KHz amplitude; 0.2 G modulation; 81.920 ms conversion time; and 81.920 ms time constant. Processing of EPR spectra (digital filtering, baseline correction, splittings, etc.) was performed using Bruker WIN-EPR software.

Molecular modeling

Computer-assisted molecular modeling was performed using the MacMimic 3.0 program (version 3.0; InStar Software, Lund, Sweden) running on a Power Macintosh 7600/120 workstation. AM1 semiempirical and ab initio calculations were performed using the MacSpartan Plus 1.0 program (version 1.0; Wavefunction, Irvine, CA) running on a Macintosh Quadra950 workstation equipped with an Apple Power Macintosh Upgrade Card or on a Power Macintosh 7600/120 workstation.

Theoretical calculation of intercharge distances

The intercharge distances between the charged functional group of a small target molecule and the charged functional group of the nitroxide probe were estimated by molecular modeling using the MacMimic 3.0 program. Ethyl ammonium cation and 4-amino TEMPO were utilized in this study. A dummy atom reference point was installed in the center of a triangle defined by the three hydrogen atoms of the ammonium groups in both molecules. The oxygen atom of the nitroxide ($NO^{\bullet}$) moiety was manually aligned close to the α- or β-protons in a manner such that the nitroxide oxygen and target molecule proton van der Waals surfaces were in contact. The nitroxide was placed in 50 different random alignments, giving rise to 50 different distances measured between the above-mentioned dummy atom reference points. The interammonium ion distances were then averaged. The diastereotopic protons of the methyl group were modeled separately, and the resulting 100 measured distances were averaged.

Theoretical calculation of local electrostatic potential

The electrostatic potential (EP) around specific protons calculated from computer-assisted molecular models is designated as $U(R_0)_{calc}$, and the corresponding electrostatic potential calculated from experimental data is designated as $U(R_0)_{exptl}$. The $U(R_0)_{calc}$ parameter is calculated according to the following procedure:

Step 1: Geometry optimization by a semiempirical (AM1) calculation.

Step 2: Single-point energy ab initio calculation using the 321-G* basis set Hartree-Fock method.

Step 3: An electron isodensity surface (0.002 electrons/au^3) ($\approx$ 1.2 Å) (van der Waals radius) from protons (Francl et al., 1984) was generated, and the electrostatic potential was mapped on the surface (Kahn et al., 1986). In an arbitrary but consistent manner, the molecule was oriented so that the z axis (perpendicular to the monitor screen) coincided with the C-H bond when viewed from the H-atom direction. The sterically accessible curved van der Waals surface for that particular proton now faced the viewer, and the average electrostatic potential value estimated in the vicinity of the proton was calculated from 17 sampling measurements within this accessible surface (e.g., one straight-on and four in each direction: top, bottom, right, and left). Using the classical physics formula for EP, $U(R_0) = q/\epsilon R_0$, where $U(R_0)$ is the electrostatic potential, q is the charge on specific proton, R_0 is the closest distance between the charged moiety in the nitroxide probe and the charge on the atom in the target molecule, and ϵ is the dielectric constant of the medium, the averaged EP was then corrected $[U(R_0)]$ to the dielectric constant of water ($\epsilon_{water} = 80$) and a distance of 8 Å.

Calculation of apparent local electrostatic potential and charges from experimental data

Slopes, $k_i = d(1/T_1)/d([R^{\bullet}])$, of the experimental dependence of proton spin-lattice relaxation rate on concentration of the nitroxide probes $[R^{\bullet}]$ have been measured:

$$k_i = \frac{1/T_1}{[R^{\bullet}]} \tag{1}$$

The subscripted descriptive index $i = 0$, $+1$ or -1 is utilized for data acquired from radical probes of 0, $+1$ or -1 charge, respectively. Variable k_i has the dimensions of a second-order rate constant ($M^{-1}\ s^{-1}$) and can be considered as an apparent relaxation rate constant.

According to a number of workers (Hwang and Freed, 1975; Alexandrov, 1975; Berdnikov et al., 1980), the spin-lattice relaxation rate of proton nuclei, $1/T_{1(n)}$, upon an encounter with the radical free electron, may be described by

$$1/T_{1n} = \left(\frac{4\pi}{9}\right)\left(\frac{\gamma_n^2\gamma_e^2h^2}{(R_0')^6}\right)S(S+1)T_{1e}[R^{\bullet}]f(y) \tag{2}$$

$$f(y) = \frac{(4+y)y^2}{9+9y+4y^2+y^3} \tag{3}$$

where γ_n and γ_e are the gyromagnetic ratios of protons and electrons, respectively; R_0' is the distance between proton and electron (the subscripted zero for the R' descriptor signifies that this is the closest approach distance); $[R^{\bullet}]$ is the radical concentration; $\tau_d = R_0'^2/D$, $y = (\tau_d/T_{1(e)})^{1/2}$; $T_{1(e)}$ is the spin-lattice relaxation rate of the electron; D is the sum of diffusion coefficients of the proton-bearer and radical; and S is the spin of the electron. Because of the low value of γ_n, estimations have shown (Alexandrov, 1975; Berdnikov et al., 1980) that Eq. 2 is correct at any reasonable viscosity for the medium.

In room temperature aqueous solutions of low-molecular-mass molecules, τ_d is 10^{-10} to 10^{-11} s, and $T_{1(e)}$ is 10^{-6} s for a nitroxide radical (Kolilov and Likhtenshtein, 1972, 1977; Likhtenshtein, 1993). Using these values, Eq. 1 for uncharged particles can now be expressed as

$$\left(\frac{1}{T_{1(n)}}\right)_0 = k_0[R^{\bullet}] \tag{4}$$

$$k_0 = \left(\frac{16\pi}{81}\right)\left(\frac{\gamma_n^2\gamma_e^2h^2}{(R_0')^6}\right)S(S+1)\tau_d \tag{5}$$

where k_0 is the T_1 apparent rate constant determined by experiment for neutral nitroxide (Scheme **I**).

Nitroxide radicals (Schemes **I–III**) all have similar chemical structures. They differ in the presence or absence of a small size functional group in a ring position remote from the paramagnetic nitroxide group. Therefore, it is obvious that they have very similar paramagnetic parameters according to Eq. 2. On the basis of analysis of molecular models for these radicals, we can suggest that R_0' and the diffusion coefficients of the radicals, and, therefore τ_d, are very comparable for all radicals used in this study. The

only marked difference expected for the radicals is the value and sign of their electrostatic charge (0, −1 and +1) for the corresponding radicals (Schemes **I–III**).

To explore the effect of electrostatic interaction on the dipole-dipole relaxation rate, $1/T_{1(n)}$, we employed the modified Debye-Hückel theory (Hwang et al., 1973; Hwang and Freed, 1975):

$$\beta_{el} = \frac{e^{U(R_0)/kT}}{\int_{R_0}^{\infty} \frac{e^{U(R)/kT} dR}{R^2}} \quad (6)$$

This provides a reasonable approximation for the β_{el} electrostatic term, which takes into account the contribution of electrostatic attraction or repulsion to the spin-lattice relaxation rate. In Eq. 6, the electrostatic potential at the R_0 distance of closest approach, $U(R_0)$, appears in the numerator, and the denominator describes the integral of the $U(R)$ electrostatic interaction effect over far-to-short R distances.

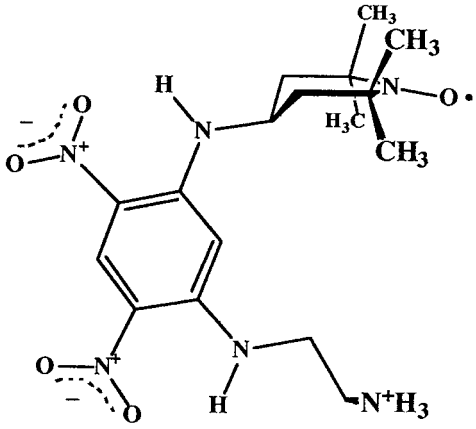

Scheme **IV**.

In the encounter complex, the R_0 closest approach distance between the charge on the atom in the target molecule and that on the charged moiety in 4-substituted-TEMPO nitroxide spin labels (Schemes **II**, **III**) is the sum of two components: the intermolecular R_0' distance of closest approach between the spin label electron and the target molecule proton plus the intramolecular R_0'' distance between the nitroxide oxygen and the charged moiety in the 4-substituent. The intramolecular R_0'' distance was estimated from the x-ray crystallographically determined structure of an *N*-substituted 4-amino-TEMPO spin-labeled hapten (Scheme **IV**) found in a hapten/antibody complex with the Fab fragment of the murine monoclonal antidinitrophenyl antibody (Brunger et al., 1991). For example, in the encounter complex, a ~7.8-Å R_0 distance between the 4-ammonium nitrogen in Scheme **III** and a proton residing in a charged environment of the target molecule may be estimated by adding the 2.4 Å sum of nitroxide-oxygen and target molecule hydrogen van der Waal radii (intermolecular R_0' closest approach distance) to the 5.4 Å intramolecular R_0'' distance measured between 4-amino nitrogen and the nitroxide-oxygen in the experimentally determined structure of Scheme **IV**.

The integral appearing in the denominator of Eq. 6 was solved, and the resulting relationship was then converted into a more readily solvable equation:

$$\beta_{el} = \frac{(U(R_0)/0.6)\, e^{U(R_0)/0.6}}{1 - e^{U(R_0)/0.6}} \quad (7)$$

A correction factor (Moelwyn-Hughes, 1961) for the ionic strength effect (β_I) is provided by

$$\beta_I = 10^{\sqrt{I}/(1+\sqrt{I})} \quad (8)$$

where I is the ionic strength.

Taking Eqs. 1–5 into consideration, the ratio of experimental apparent rate constants k_+/k_0 or k_-/k_0 can be given as

$$\frac{k_{+-}}{k_0} = \beta_{el}\beta_I \quad (9)$$

Uncertainties in β_{el} were calculated based on the experimental uncertainties in the T_1 relaxation rate constants measured by NMR spectroscopy. The estimated electrostatic potential in the vicinity of a particular proton in the target molecule based upon these T_1 apparent rate constants ($U(R_0) = U(R_0)_{exptl}$) was calculated in the following manner. The ionic strength effect correction factor (β_I) was first calculated for the particular solvent using Eq. 8, and then was utilized in Eq. 9 to calculate the electrostatic term (β_{el}) from the T_1 apparent rate constant ratios k_+/k_0 and k_-/k_0. Using β_{el}, $U(R_0)_{exptl}$ can now be calculated from Eq. 7.

These $U(R_0)_{exptl}$ values can be compared with the $U(R_0)_{calc}$ theoretically expected values determined from molecular modeling. The apparent dielectric constant ϵ_{app} for the charged probe-protonated imidazole encounter complex can be derived from

$$\epsilon_{app} = \frac{U(R_0)_{exp}}{\epsilon_{water} U(R_0)_{calc}} \quad (10)$$

This is based on the assumption that the average distance R_0 in the actual complex is similar in the molecular model, and $\epsilon_{water} = 80$.

The electrostatic effect in the vicinity of a proton coming from charged functional groups (ammonium cation, carboxylate anion, etc.) in other regions of a target molecule X can be quantitatively characterized in an empirical manner by a relative apparent charge, α^x:

$$\alpha^x = \frac{Z^x_{app}}{Z^0} = \frac{U(R_0)^x_{exp\ tl}}{U(R_0)^0_{exp\ tl}} \quad (11)$$

where descriptive indexes x or 0 are assigned to a generic target molecule or to a small charged model compound (ethylammonium cation, imidazolium cation, propionate anion, etc.), respectively. The α^x value will be dependent on the position of the proton in the target molecule relative to the neighboring charged group. Taking $Z_0 = +1$ or -1, we can consider $Z^x_{app} = \alpha^x$ to be a parameter indicating an electrostatic effect of the molecule on a charged particle placed in the vicinity of a given proton. Such a parameter can be used in the analysis of electrostatic factors affecting equilibrium and reaction rate constants for nuclei residing in particular local charge environments within the molecule.

RESULTS

The spin-lattice relaxation rate ($1/T_1$) of protons in small target molecules (aliphatic alcohols (ethanol, isopropanol, *tert*-butanol), benzyl alcohol, propionate anion, ethylammonium cation, imidazolium cation) and amino acids (glycine, aspartic acid, histidine, and lysine) were measured as a function of concentration of spin probes with different charges. In each case, $1/T_1$ was found to be proportional to the probe concentration, as expected from Eq. 1. The slopes (apparent rate constants, k_i, from the above-mentioned experimental dependence of proton spin-lattice relaxation rate on concentration, [R•], of the different charged nitroxide probes) were then calculated. The values for neutral small molecules are reported in Table 1, and those for charged small molecules and amino acids are given in Table 2. Figs. 1–3 are graphs of some of the above results and illustrate the effect of nitroxide spin probe concentration upon $1/T_1$ for different protons in neutral small molecules, an ammonium

TABLE 1 Apparent rate constants (k_0, k_-, k_+) calculated from the experimental T_1 data acquired for different protons in neutral molecules

Molecule	Proton	δ*	k_0[#]	k_-[§]	k_+[¶]
Ethanol	H(α)	3.6	187 ± 13		
Ethanol	H(β)	1.1	165 ± 21		
Isopropanol	H(α)	3.9	168 ± 6		
Isopropanol	H(β)	1.1	149 ± 13		
Tertiary-butanol	H(β)	1.2	158 ± 17	170 ± 5	155 ± 11
Benzyl alcohol	H(α)	4.6	194 ± 29		
Benzyl alcohol	H(Ar)	7.2–7.4	195(6) ± 6[‖]		

*Ppm downfield from tetramethylsilane.
[#]Nitroxide = 4-hydroxy-TEMPO, M^{-1} s^{-1}.
[§]Nitroxide = 4-carboxy-TEMPO, M^{-1} s^{-1}, solution pD adjusted to ~7.
[¶]Nitroxide = 4-amino-TEMPO, M^{-1} s^{-1}, solution pD adjusted to ~4.
[‖]Estimated standard deviation of the mean value given in parenthesis.

cation, a carboxylate anion, as well as a basic and an acidic amino acid. Inspection of the representative graphs and the k_i values in Table 1 demonstrates that the slopes of $d(1/T_1)/d([R^{\bullet}]) = k_i$ for specific protons in charged small molecules (and in acidic and basic amino acids) are sensitive to the nitroxide spin probe (Schemes **I–III**) charge type relative to that in the charged target molecule. Thus steeper slopes were observed for spin probes of opposite charge type, shallower slopes were noted for probes with the same charge type, and intermediate slopes were found for neutral probes. The contribution of the nitroxide spin probe to the spin-lattice relaxation rate of specific target molecule protons may be given by $\Delta(1/T_1) = (1/T_1)_x - (1/T_1)_0$, where $(1/T_1)_x$ and $(1/T_1)_0$ are the spin-lattice relaxation rates in the presence and absence of nitroxide, respectively. The $(1/T_1)_0$ rate parameter is the *y*-intercept in Figs. 1–3.

In the case of studies with the neutral probe (Scheme **I**), the average k_0 for all of the protons in three representative aliphatic alcohols (ethanol, isopropanol, and *tert*-butanol) is equal to 165(12) M^{-1} s^{-1} (estimated standard deviation given in parenthesis; see Fig. 1). Differences in k_0 among the alcohols and between the H(α) and H(β) protons are all

TABLE 2 Apparent rate constants (k_0, k_-, k_+) calculated from the experimental T_1 data acquired for different protons in small charged molecules and amino acids*

Molecule	Proton	δ[#]	k_0[§]	k_-[¶]	k_+[‖]
$EtNH_3]^+Cl^-$	H(α)	2.9	126 ± 11	182 ± 4	69 ± 2
$EtNH_3]^+Cl^-$	H(β)	1.1	142 ± 14	189 ± 2	81 ± 4
Imidazolium$^+Cl^-$	H(2)	7.6	129 ± 23	245 ± 12**	87 ± 8
Imidazolium$^+Cl^-$	H(4,5)	7.0	140 ± 13	251 ± 13**	89 ± 9
$EtCO_2$-Na^+	H(α)	2.1	143 ± 14[##]	81 ± 11	225 ± 29[§§]
$EtCO_2$-Na^+	H(β)	1.0	125 ± 17[##]	87 ± 9	200 ± 18[§§]
Glycine	H(α)	3.5	118 ± 9	112 ± 11	132 ± 7
Aspartic Acid	H(α)	3.8	155(15) $n = 5$	89(12) $n = 4$	219(25) $n = 2$
Aspartic Acid	H(β_I)	2.6	131(14) $n = 5$	67(9) $n = 4$	178(8) $n = 2$
Aspartic Acid	H(β_{II})	2.7	130(10) $n = 5$	66(11) $n = 4$	187(9) $n = 2$
Histidine	H(α)	4.0	162 ± 22		108 ± 10
Histidine	H($\beta_{I,II}$)	3.1	161 ± 36		107 ± 15
Histidine	H(2)	8.5	180 ± 8		99 ± 12
Histidine	H(4)	7.5	183 ± 5		96 ± 11
Lysine	H(α)	3.7	153 ± 10		105 ± 1
Lysine	H($\beta_{I,II}$)	1.8	131 ± 15		104 ± 17
Lysine	H($\gamma_{I,II}$)	1.3	162 ± 19		98 ± 3
Lysine	H($\delta_{I,II}$)	1.6	135 ± 15		98 ± 1
Lysine	H(ε)	2.9	147 ± 18		91 ± 2

*Plus/minus denotes the average deviation from the least-squares straight line apparent rate constant slope in a plot of T_1^{-1} versus five concentrations of radical, while parentheses show the standard deviation in the mean of *n* independent determinations of the apparent rate constant slope.
[#]Ppm downfield from tetramethylsilane.
[§]Nitroxide = 4-hydroxy-TEMPO, M^{-1} s^{-1}.
[¶]Nitroxide = 4-carboxy-TEMPO, M^{-1} s^{-1}, solution pD adjusted to ~7 (unless noted otherwise).
[‖]Nitoxide = 4-amino-TEMPO, M^{-1} s^{-1}, solution pD adjusted to ~4 (unless noted otherwise).
**Solution pD adjusted to ~5.
[##]Solution pD adjusted to ~6.
[§§]Solution pD adjusted to ~7.

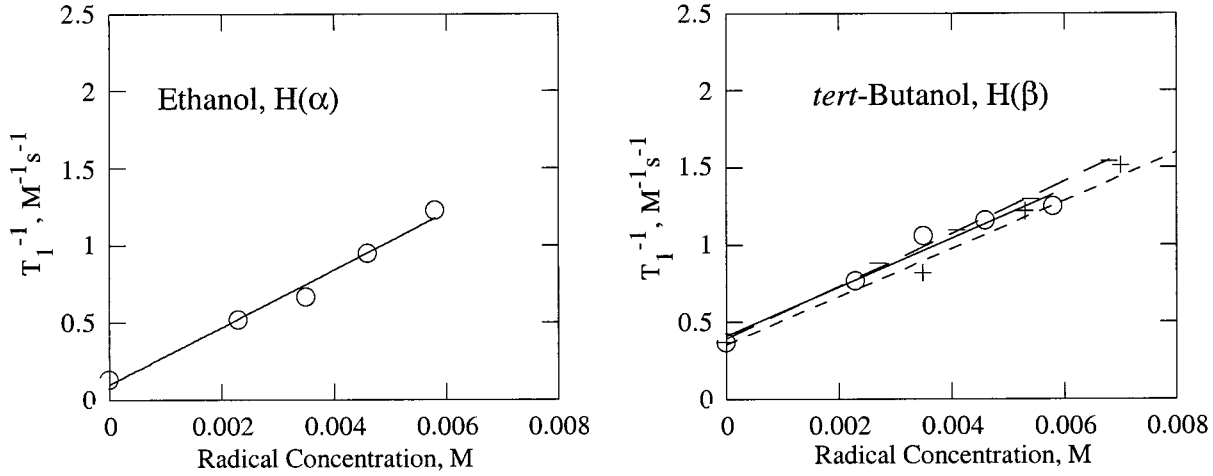

FIGURE 1 Spin lattice relaxation rates ($1/T_1$) of small neutral molecules (ethanol and *tert*-butanol) as a function of spin probe radical concentration. Neutral, negative, and positive charged spin probes are respectively denoted as ○, −, and +.

within the experimental error in determining the k_0 slope. Similarly, k_0 for benzyl alcohol H(α) protons also appears not to be significantly different in magnitude from the values for protons in aliphatic alcohols, whereas the k_0 for benzyl alcohol H(aromatic)$_{av}$ appears to be only very slightly higher (195(6) M^{-1} s^{-1}). For small charged molecules, the k_0 values for protons in propionate anion (143 ± 14 M^{-1} s^{-1}, H(α)) (see Fig. 2), ethylammonium cation (134(11), H(α, β)$_{av}$ M^{-1} s^{-1}), and imidazolium cation (135(8), H(2, 4, 5)$_{av}$ M^{-1} s^{-1}) (see Fig. 2) were found to be quite similar and within the experimental error of their determination. Their values are only very slightly lower than those for protons in alcohols. The apparent k_0 constants for charged amino acids, obtained using neutral probe (Scheme **I**), were found to be within a range of 131–162 M^{-1} s^{-1} for H(aliphatic) and are equal to 180–183 M^{-1} s^{-1} for the histidine imidazole ring protons (see Fig. 3). In general, the reproducibility of these experimentally determined apparent rate constants were found to be very satisfactory. For example, three determinations of k_0 for aspartic acid afforded values of 162(15) [H(α)], 140(7) [H(β_I)], and 136(7) [H(β_{II})], and two determinations of k_- gave 99(5) [H(α)], 75(1) [H(β_I)], and 75(5) [H(β_{II})]. Neutral small molecules were insensitive to the charge type of the nitroxide spin probe, as expected. For example, the k_i values for *tert*-butanol protons were all very similar and were within the experimental error of their measurement: 158 ± 17 [k_0], 170 ± 5 [k_-], 155 ± 11 [k_+], and the average of these three values is 161(8).

More marked differences in the k_i values were found experimentally for systems containing both a charged probe and a charged target molecule (Figs. 2 and 3 and Table 2). The k_-/k_0 and k_0/k_+ ratios (for positively charged target molecules, or k_+/k_0 and k_0/k_- ratios for negatively charged ones) are in the range of 1.33–1.90, and we have already shown that those for small neutral molecules are essentially

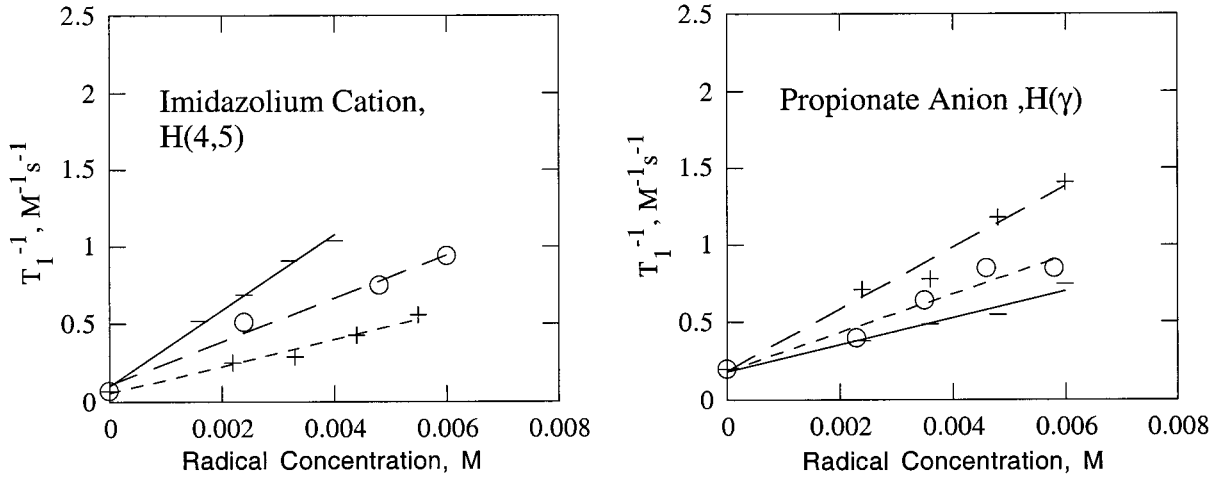

FIGURE 2 Spin lattice relaxation rates ($1/T_1$) of small charged molecules (imidazolium cation and propionate anion) as a function of spin probe radical concentration. Neutral, negative, and positive charged spin probes are respectively denoted as ○, −, and +.

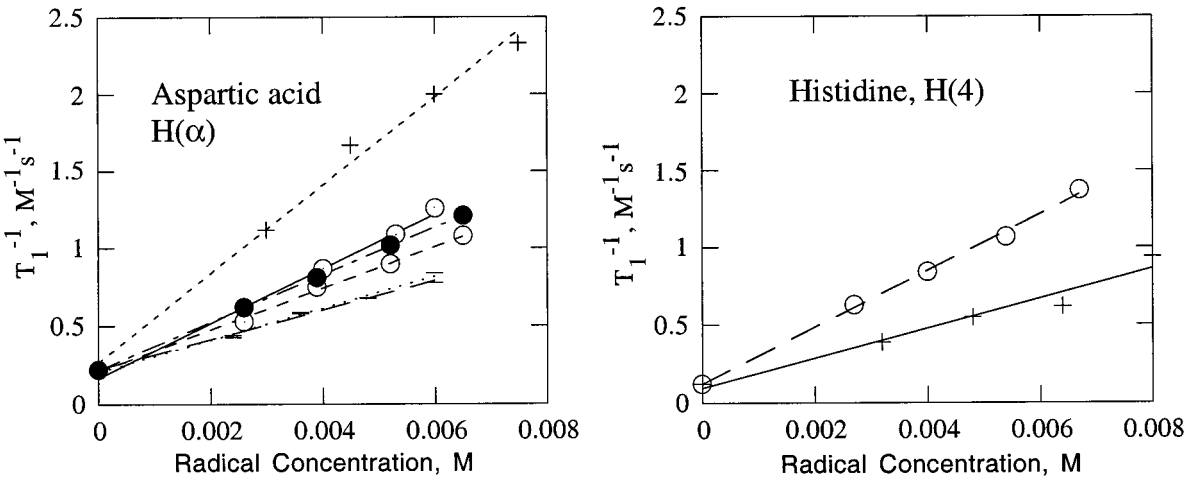

FIGURE 3 Spin lattice relaxation rates ($1/T_1$) of acidic and basic amino acids (aspartic acid and histidine) as a function of spin probe radical concentration. Neutral, negative, and positive charged spin probes are respectively denoted as ○, −, and +.

unity, as expected. Moreover, they are reasonable, because they qualitatively agree with values expected for electrostatic interactions, namely, attraction for groups of different charges and repulsion for those bearing the same charges.

The sensitivity to spin probe charge type experienced by nuclei within charged target molecules is clearly evident upon perusal of the larger magnitude (2.30–3.82) k_-/k_+ or k_+/k_- ratios calculated for systems amenable for investigation under conditions in which both the negative and positively charged spin probes and the functional group within the target molecule were all ionized under appropriate pD conditions. Most but not all of the cases could be studied in this manner. For those that could not, only the relatively lower magnitude k_-/k_0 or k_0/k_+ ratios could be calculated.

1. For the protonated imidazolium cation, and for the protonated imidazole ring as a fragment of histidine, the average k_-/k_0 or k_0/k_+ ratios for protons therein are both 1.7(2). These respective average ratios were found to be only very slightly smaller (1.50) for the histidinyl aliphatic H(α,β). Using the more charge-sensitive k_-/k_+ ratios calculated for imidazolium cation ring protons, the average value of 2.82 signifies a marked effect of probe charge type on the T_1 relaxation rate of protons therein. Similarly, the H(α) and H(β) nuclei of ethylammonium cation afford k_-/k_+ ratios of 2.64 and 2.33, respectively.

2. The opposite charge type of the propionate anion (compared to the cations above) is clearly indicated by the 2.78 and 2.30 inverse k_-/k_+ ratios (i.e., k_+/k_-) calculated for respective H(α) and H(β) nuclei therein.

3. Differences in k_0 values for the protonated lysine side-chain protons are not significant because they all fall within the error of their determinations. A similar observation can be made for the k_+ values of this molecule. The side-chain protons clearly experience a positively charged environment, as shown by an average k_0/k_+ ratio of 1.46(16) for these nuclei. This average value is smaller than that measured for protons in ethylammonium cation and might be due to partial "quenching" by the neighboring negatively charged carboxylate anion, which can sterically interact with the positive protonated amino groups. As in the case of propionate anion, the average 2.66, 2.83, and 2.46 inverse k_-/k_+ ratios (i.e., $k_{+(av)}/k_{-(av)}$) calculated for respective H(β_I), H(β_{II}), and H(α) protons in aspartate (e.g., see Fig. 3) clearly show residence in negatively charged surroundings. Comparison of H(β_I) and H(β_{II}) $k_{+(av)}/k_{-(av)}$ values shows them to be within the experimental error. Although these two diastereotopic aspartic acid methylene protons are expectedly anisochronous in their chemical shift values, subtle differences in the electrostatic environments of their weighted time-averaged conformation are apparently too small to be measured by the spin probes. Although H($\beta_{I,II}$) $k_{+(av)}/k_{-(av)}$ values are slightly larger than that for H(α), it is unclear whether the magnitude of this difference is significant.

4. Not surprisingly, the 1.05 k_0/k_-, 1.12 k_+/k_0, and 1.18 k_+/k_- ratios for glycine H(α) protons were found to be essentially the same.

The molecular modeling calculation of local electrostatic potential described in Materials and Methods was applied to a number of small charged (ethylamine, propionate anion, and imidazole) and uncharged (ethanol) molecules. Using dielectric constants $\epsilon = 1$ and 80 for the media, theoretical values of the electrostatic potential $U(R_0)_{calc}$ were calculated for $R = 1$ and 8 Å distances between charged groups of probes, Schemes **II** or **III**, and the specific protons in the molecules under investigation. These values are presented in Table 3. Using the T_1 NMR data, the apparent electrostatic potentials $U(R_0)_{exptl}$, calculated with the use of Eqs. 6, 9, and 11, are also presented in the table.

DISCUSSION

The simple organic molecules and amino acids in these investigations provide well-defined molecules for the study

TABLE 3 Electrostatic potentials $U(R_0)_{calcd}$ estimated from sampling the accessible 1.2 Å radius van der Waals surface in the vicinity of different protons of charged molecules using ab-initio calculated molecular models (diaelectric constant of $\epsilon = 1$), and then calculated for a dialectric constant of 80 and 8 Å radius versus electrostatic potentials $U(R_0)_{exptl}$ calculated from the experimental T_1 data measured in D_2O.

Molecule	Proton	$U(R_0)_{calcd}$*,# $\epsilon = 1$, $R = 1.2$ Å	$U(R_0)_{calcd}$* $\epsilon = 80$, $R = 8$ Å	$U(R_0)_{exptl}$*,#,§
Ethanol	H(α)	15(1)	+0.03	
Ethanol	H(β)	10(1)	+0.02	
$EtNH_3]^+Cl^-$	H(α)	126(2)	+0.25	+0.29(6)¶
$EtHN_3]^+Cl^-$	H(β)	109(4)	+0.22	+0.26(8)
Imidazolium$^+Cl^-$	H(2)	151(3)	+0.30	+0.30(8)¶
Imidazolium$^+Cl^-$	H(4,5)	130(3)	+0.26	+0.30(4)¶
$EtCO_2$-Na^+	H(α)	−80(4)	−0.16	−0.29(3)‖
$EtCO_2$-Na^+	H(β)	−71(3)	−0.14	−0.26(4)‖
Aspartate-Na^+	H(α)			−0.30(5)¶
Aspartate-Na^+	H(β)			−0.31(6)¶

*Kcal mol^{-1}.
#Estimated standard deviation of last digit given in parenthesis.
§Average of apparent electrostatic potentials calculated separately from k_+/k_0 ratios and k_0/k ratios for negatively charged molecules, or from k_-/k_0 and k_0/k_+ ratios for positively charged molecules.
¶$I = 0.008$, $\beta_I = 1.20$.
‖$I = 0.013$, $\beta_I = 1.26$.

of the factors that influence electrostatic fields in more complex biologically important molecules. These model systems enable us to verify our experimental and theoretical approaches to this problem. According to the theory of spin relaxation (Krugh, 1971; Hwang and Freed, 1975; Alexandrov, 1975; Berdnikov et al., 1980), the rate of the proton spin-lattice relaxation in the presence of paramagnetic molecules depends upon a number of factors (e.g., the distance between the spins in the encounter complex, the correlation time of dipole-dipole interactions, the magnetic moment of paramagnetic species (Eqs. 2–6), and electrostatic charges, if present). Because the only essential difference in the nitroxide spin probes, Schemes **I–III**, in our experiments is the difference in charges Z_p and the distances between these charges and charges Z_x in molecules under investigation, then the ratio of the apparent spin-lattice relaxation rate constants (Table 2) is, in fact, a quantitative parameter taking into account the effect of electrostatics upon the encounter interaction (see Eqs. 7–10). Measurement of this parameter allows one to calculate an NMR-based average electrostatic potential $U(R_0)_{exptl}$ between the charged probe and a given target molecule proton and then to compare it with the theoretical one $U(R_0)_{calc}$ based upon molecular modeling.

The apparent rate constant k_0 (Eq. 4) is a quantitative characteristic of the effect of a neutral nitroxide probe (Scheme **I**) on the proton lattice relaxation rate $(1/T_1)$ of molecules under investigation. If one carefully compares the k_0 values in Tables 1 and 2, it is apparent that these do not show significant differences relative to the errors in their experimental determinations. Other reasons for their differences might reflect relatively weak specific interactions between a molecule under investigation and the probe: for example, the formation of a hydrogen bond between the probe hydroxyl and a charged or hydroxyl group in the target molecule, or a short-lived nitroxide-phenyl ring donor-acceptor pair, which may exert a small affect upon the effective correlation time τ_d (Eq. 2).

On the other hand, the values for apparent k_+ and k_- rate constants of spin-lattice relaxation for specific protons of charged small molecules and amino acids listed in Table 2 clearly show that the apparent electrostatic potentials $U(R_0)_{exptl}$ around these nuclei in the solution state are dependent upon the charge of the particular nitroxide spin probe as well as on the charge of neighboring functional groups. However, it remains to be shown whether this method will be sensitive enough to ascertain subtle effects arising from the position of a proton nucleus relative to the neighboring charged functional group in molecules having conformational inhomogeniety.

In a test study, differences between the apparent electrostatic potential $U(R_0)_{exptl}$ for α- and β-protons in the same small target molecule fell within the experimental error. The averaged intercharge distances between charged functional groups on the small ethyl ammonium cation target molecule and that on the 4-amino TEMPO nitroxide probe, measured by molecular modeling for various alignments of the nitroxide oxygen with α- or β-protons in the target molecule, were calculated (as explained Materials and Methods). These averaged distances between the two ammonium ions were found to be 10.5(6) and 11.1(4) Å, using nitroxide contact with the α- or β-protons in the target molecule, respectively. The difference between these two values is insignificant, and this can account for the difficulty in experimentally detecting significantly different electrostatic potentials around specific protons in small flexible target molecules.

The k_-/k_+ ratios for ammonium cation charged target molecules (or the k_+/k_- ratios for those with carboxylate anions) calculated from the values listed in Tables 1 and 2 were found to range from 2.3 to 2.9. In other words, in the

series of charged compounds studied in this work, the apparent spin-lattice relaxation rates for nuclei under the influence of electrostatic forces involving the spin probe are approximately two to three times higher compared to those for nuclei in neutral molecules. These values are significantly higher than the 0.8–1.2 ratio n obtained with systems containing the uncharged probe, Scheme **I**, and charged small molecules or charged amino acids. In each case, comparison of data with the three probes, Schemes **I–III**, shows that the sign of the nitroxide probe electrostatic charge and of the target molecule determines the relative pitch (steepness) of the slopes, $d(1/T_1)/d[R^{\cdot}]$, for the experimental dependence of $1/T_1$ as a function of the concentration of the particular nitroxide. For positively charged target molecules, we have found that $k_+ < k_0 < k_-$, whereas for negatively charged molecules, $k_+ > k_0 > k_-$.

As one can see from Tables 1–3, the sign and magnitudes of both parameters $U(R_0)_{exptl}$ and $U(R_0)_{calc}$ correspond to expected values from simple electrostatic considerations. The sign is positive for protonated ethylamine and imidazole and negative for propionate anion. The absolute value of $U(R_0)_{calc}$ is very small for protons in neutral ethanol and is markedly larger for those in small charged molecules (propionate anion, ethylammonium cation, and imidazolium cation). Comparison of $U(R_0)_{exptl}$ with $U(R_0)_{calc}$ values for protonated imidazole (Eq. 10) shows them to be in quantitative agreement (see Table 3) if the apparent dielectric constant is taken as $\epsilon_{app} = 56$.

We propose that the value of $U(R_0)_{calc}$ and the apparent electrostatic charge $Z_{0app} = \pm 1$ (Eq. 11) for small charged molecules can be used as standards in investigations of more complex molecules bearing appropriate electrostatic charges. A deviation of $U(R_0)_{exptl}$ and Z_{xapp} for a proton in such a molecule from values for standard molecules can indicate the sign and magnitude of electrostatic effects in various regions of the molecule under investigation.

The general conclusions from this study are as follows:

1. Proton nuclei located at different positions within the small molecules and amino acids that were investigated exhibit similar degrees of spin probe accessibility, as shown by the similar values of slope $d(1/T_1)/d[R^{\cdot}]$ for these protons in the presence of the neutral spin probe **I**. This experimental observation is consistent with the theoretical estimation of spin probe accessibility as studied by computer-assisted molecular modeling of the various amino acid/spin probe encounter complexes in our study.

2. In small charged molecules and in charged amino acids, the charge of functional groups and their charge type clearly result in local electrostatic potentials experienced by neighboring nuclei and are amenable to solution-state investigation by charged nitroxide spin probes. These local electrostatic potentials appear to be concentrated around the ionized functional group in aspartic acid, whereas the results for more conformationally heterogeneous histidine and lysine show noticeable local electrostatic charged fields around proton nuclei located some distance from the functional groups.

3. The method used in this investigation did not reveal a local electrostatic potential for the glycine α-H nuclei located close to the zwitterionic environment.

The above-mentioned results illustrate the reliability of the new technique that was utilized in these investigations and show that it has the potential for development into a method for the quantitative study of local charge distribution in polypeptides and proteins. Although the differently charged spin probes have been used so far on only a rather limited number of examples reported herein, the results show that this new methodology shows great promise for the investigation of local electrostatic fields in a wide range of biologically important molecules.

EPR and NMR experiments were performed at The University Laboratory for Magnetic Resonance (Ben-Gurion University of the Negev).

The Bruker DMX-500 spectrometer was purchased with a matching funds grant from the Israel Ministry of Science and Industry.

REFERENCES

Alexandrov, I. V. 1975. Theory of Magnetic Relaxation. Nauka, Moscow.

Anni, H., J. M. Vanderkooi, K. A. Sharp, T. Yonetani, S. C. Hopkins, L. Herenyi, and J. Fidy. 1994. Electric field and conformational effects of cytochrome c and solvent on cytochrome c peroxidase studied by high resolution fluorescence spectroscopy. *Biochemistry.* 33:3475–3486.

Aqvist, J., H. Luecke, F. A. Quiocho, and A. Warshel. 1991. Dipoles localized at helix termini of proteins stabilize charges. *Proc. Natl. Acad. Sci. USA.* 88:2026–2030.

Bajorath, J., D. H. Kitson, J. Kraut, and A. T. Hagler. 1991. The electrostatic potential of *Escherichia coli* dihydrofolate reductase. *Proteins.* 11:1–12.

Bashford, D., and K. Gerwert. 1992. Electrostatic calculations of the pK_a values of ionizable groups in bacteriorhodopsin. *J. Mol. Biol.* 224: 473–486.

Bashford, D., and M. Karplus. 1990. pK_as of ionizable groups in proteins: atomic detail from a continuum electrostatic model. *Biochemistry.* 29: 10219–10225.

Berdnikov, B. M., A. B. Doctorov, and L. L. Makarshin. 1980. Dipole-dipole broadening of free radicals ESR spectra in the presence of paramagnetic ions. *Theor. Exp. Chem. (Kiev).* 16:765–771.

Beroza, P., D. R. Fredkin, M. Y. Okamura, and G. Feher. 1991. Protonation of interacting residues in a protein by a Monte Carlo method: application to lysozyme and the photosynthetic reaction center of *Rhodobacter sphaeroides*. *Proc. Natl. Acad. Sci. USA.* 88:5844–5808.

Borah, B., and R. G. Bryant. 1981. Nuclear magnetic resonance relaxation dispersion in an aqueous nitroxide system. *J. Chem. Phys.* 75: 3297–3300.

Brooks, B. R., R. E. Bruccolery, B. D. Olafson, D. J. States, S. Swaminathan, and M. Karplus. 1983. CHARMM: a program for macromolecular energy, minimization, and dynamics calculations. *J. Comput. Chem.* 4:187–217.

Brunger, A. T., D. J. Leahy, T. R. Hynes, and R. O. Fox. 1991. 2.9 Ångstroms resolution structure of an anti-dinitrophenyl-spin-label monoclonal antibody Fab fragment with bound hapten. *J. Mol. Biol.* 221:239–256.

Daggett, V. D., P. A. Kollman, and I. D. Kuntz. 1989. Free energy perturbation calculations of charge interactions with the helix dipole. *Chem. Script.* 29A:205–215.

Druzhinin, S. Yu., V. R. Fogel, L. A. Syrtzova, G. I. Likhtenshtein, and A. I. Kotelnikov. 1986. Study on the cofactor center localization in nitrogenase by triplet labeling method. *Biophysics.* 31:16–21.

Dwek, R. A. 1972. Proton relaxation enhancement probes. *Adv. Mol. Rel. Proc.* V:1–53.

Francl, M. M., R. F. Hout, Jr., and W. J. Hehre. 1984. Representation of electron densities. 1. Sphere fits to total electron density surfaces. *J. Am. Chem. Soc.* 106:563–570.

Freeman, R., and H. D. W. Hill. 1969. High-resolution studies of nuclear spin-lattice relaxation. *J. Chem. Phys.* 224:3140–3145.

Gilson, M. K. 1993. Multiple-site titration and molecular modeling: two rapid methods for computing energies and forces for ionizable groups in proteins. *Proteins.* 15:266–282.

Gilson, M. K., and B. H. Honig. 1988. Energetic of charge-charge interactions in proteins. *Proteins.* 3:32–52.

Gilson, M. K., A. Rashin, R. Fine, and B. Honig. 1985. On the calculation of electrostatic interactions in proteins. *J. Mol. Biol.* 184:503–516.

Gilson, M. K., A. Sharp, and B. Honig. 1987. Calculating the electrostatic potential of molecules in solution: method and error assessment. *J. Comp. Chem.* 9:327–335.

Hao, Y., M. R. Pear, and D. D. Busath. 1997. Molecular dynamics study of free energy profiles for organic cations in gramicidin A channels. *Biophys. J.* 73:1699–1716.

Hecht, J. L., B. Honig, Y.-K. Shin, and W. L. Hubbell. 1995. Electrostatic potentials near the surface of DNA: comparing theory and experiment. *J. Phys. Chem.* 99:7782–7786.

Honig, B., and A. Nicholls. 1995. Classical electrostatics in biology and chemistry. *Science.* 268:1144–1149.

Honig, B., K. Sharp, and A.-S. Yang. 1993. Macroscopic models of aqueous solutions: biological and chemical applications. *J. Phys. Chem.* 97:1101–1109.

Hwang, L. P., and J. H. Freed. 1975. Dynamics effect of pair correlation functions on spin-relaxation by translational diffusion in liquids. *J. Chem. Phys.* 63:4017–4025.

Hwang, L. P., C. V. Krishnan, and H. L. Friedman 1973. The study of solute-solute forces by NMR relaxation. *Chem. Phys. Lett.* 20:391–393.

Ilan, Y., and A. Shafferman. 1979. Intramolecular electron transfer and binding constants in iron hexacyanide-cytochrome c complexes as studied by pulse radiolysis. *Biochim. Biophys. Acta.* 548:161–165.

Kahn, S. D., C. F. Pau, and W. J. Hehre. 1986. Modeling chemical reactivity. *J. Am. Chem. Soc.* 108:7381–7396.

Kitson, D. H., and A. T. Hagler. 1988. Theoretical studies of the structure and molecular dynamics of a peptide crystal. *Biochemistry.* 27: 5246–5257.

Klapper, I. K., R. Hagstrom, R. Fine, K. Sharp, and B. Honig. 1986. Focusing of electric fields in the active site of Cu-Zn superoxide dismutase: effects of ionic strength and amino acid modification. *Proteins.* 1:47–59.

Kopple, K. D., and A. Go. 1977. Conformation of cyclic peptides. 9. Cyclodimerization of a hexapeptide unit at high concentration. Rationalization in terms of the conformation of the cyclic dodecapeptide. *J. Am. Chem. Soc.* 99:7698–7704.

Krugh, T. R. 1971. Proximity of the nucleoside monophosphate and triphosphate binding sites on deoxyribonucleic acid polymerase. *Biochemistry.* 10:2594–2599.

Kulikov, A. V., and G. I. Likhtenshtein. 1974. Application of saturation curves for evaluating distances in biological objects by the method of double spin-labels. *Biophysika.* XIX-3:420–424.

Kulikov, A. V., and G. I. Likhtenshtein. 1977. The use of spin relaxation phenomena in the investigation of the structure of model and biological systems by the methods of spin labels. *Adv. Mol. Relax. Interact. Proc.* 10:47–77.

Lanir, A., and G. Navon. 1972. Nuclear magnetic resonance studies of carbonic anhydrase. Binding of sulfacetamide to the manganese enzyme. *Biochemistry.* 11:3536–3544.

Leniart, D. S., H. D. Connor, and J. H. Freed. 1975. An ESR and ENDOR study of spin relaxation of semiquinone in liquid solution. *J. Chem. Phys.* 63:165–199.

Lezina, V. P., A. U. Stepanyants, and G. I. Likhtenshtein. 1976. Study on the interaction of steroids with serum albumin by the NMR spin-echo technique. *Mol. Biol.* 10:1166–1175.

Likhtenshtein, G. I. 1976. Investigation of protein microstructure by the spin probe spin label method. *In* Spin Labeling Methods in Molecular Biology. USSR Academy of Sciences, Moscow, and John Wiley and Sons, New York. 67–69.

Likhtenshtein, G. I. 1988. Chemical Physics of Redox Metalloenzymes. Springer Verlag, Heidelberg.

Likhtenshtein, G. I. 1993. Biophysical Labeling Methods in Molecular Biology. Cambridge University Press, Cambridge. 67–69.

Likhtenshtein, G. I., Yu. D. Akhmedov, L. V. Ivanov, L. A. Krinitskaya, and Yu. V. Kokhanov. 1974. Investigation of the lysozyme macromolecule by a spin-labeling method. *Mol. Biol.* 8:40–48.

Likhtenshtein, G. I., V. R. Fogel, and A. V. Kotelnikov. 1985. Estimation of the electron transfer parameters in cytochrome C. *Biophysics.* 30: 394–400.

Likhtenshtein, G. I., Yu. B. Grebentchikov, P. Kh. Bobodzhanov, and Yu. V. Kokhanov. 1970. Study on the proteins microstructure by method of spin-label paramagnetic probe. *Mol. Biol.* 4:782–789.

Likhtenshtein, G. I., Yu. B. Grebentchikov, E. G. Rosantev, and V. P. Ivanov. 1972. Study on the electrostatic charges in proteins by method of paramagnetic probes. *Mol. Biol.* 6:498–507.

Lockhart, D. J., and P. S. Kim. 1992. Internal Stark effect measurement of the electric field at the amino terminus of an α-helix. *Science.* 257: 947–951.

Lockhart, D. J., and P. S. Kim. 1993. Electrostatic screening of charge and dipole interactions with the helix backbone. *Science.* 260:198–202.

Loewenthal, R., J. Sancho, T. Reinikainen, and A. R. Fersht. 1993. Long-range surface charge-charge interactions in proteins: comparison of experimental results with calculations from a theoretical method. *J. Mol. Biol.* 232:574–583.

Mildvan, A. S ., and H. Weiner. 1969. Interaction of a spin-labeled analogue of nicotinamide adenine dinucleotide with alcohol dehydrogenase. *J. Biol. Chem.* 244:2465–2475.

Moelwyn-Hughes, E. A. 1961. Physical Chemistry. Pergamon Press, New York.

Navon, G., and G. Valensin. 1987. Nuclear relaxation times as a source of structural information. *Metal Ions Biol. Syst.* 21:1–45.

Nicholson, H., D. E. Anderson, S. Dao-Pin, and B. W. Matthews. l99l. Analysis of the interaction between charged side chains, and the α-helix dipole using designed thermostable mutants of phage T4 lysozyme. *Biochemistry.* 30:9816–9828.

Niccolai, N., C. Rossi, G. Valensin, P. Mascagni, and W. A. Gibbons. 1984. An investigation of the mechanisms of nitroxide-induced proton relaxation enhancements in biopolymers. *J. Phys. Chem.* 88:5689–5692.

Niccolai, N., G. Valensin, C. Rossi, and W. A. Gibbons. 1982. The stereochemistry and dynamics of natural products and biopolymers from proton relaxation spectroscopy: spin-label delineation of inner and outer protons of gramicidin S including hydrogen bonds. *J. Am. Chem. Soc.* 104:1534–1537.

Reuben, J., and F. J. Kayne. 1971. Thallium-205 nuclear magnetic resonance study of pyruvate kinase and its substrates. *J. Biol. Chem.* 246: 6227–6234.

Roberts, G. G. K., J. Hannah, and O. Jardetzky. 1969. Noncovalent binding of a spin labeled inhibitor to ribonuclease. *Science.* 165:504–510.

Scott, D. L., A. M. Mandel, P. B. Sigler, and B. Honig. 1994. The electrostatic basis for the interfacial binding of secretory phospholipases A_2. *Biophys. J.* 67:493–504.

Sharp, K., and B. Honig. 1990. Electrostatic interactions in macromolecules: theory and applications. *Annu. Rev. Biophys. Chem.* 19:301–332.

Sharp, K., J. Jean-Charles, and B. Honig. 1992. A local dielectric constant model for solvation free energies which accounts for solute polarizability. *J. Phys. Chem.* 96:3822–3828.

Shoemaker, K. R., P. S. Kim, E. J. York, J. M. Stewart, and R. L. Baldwin. 1987. Texts of the helix dipole model for stabilization of α-helices. *Nature.* 326:563–567.

Sitkoff, D., D. J. Lockhart, K. A. Sharp, and B. Honig. 1994. Calculation of electrostatic effects at the amino terminus of an α-helix. *Biophys. J.* 67:2251–2260.

Sletten, E., J. I. Jackson, P. D. Burns, and G. N. La Mar. 1983. Effects of cross relaxation on the analysis of T 1 data in paramagnetic proteins. *J. Magn. Reson.* 52:492–496.

Sloan, D. L., and A. S. Mildvan. 1974. Magnetic resonance studies of the geometry of bound nicotinamide adenine dinucleotide and isobutyra-

mide on spin labeled alcohol dehydrogenase. *Biochemistry.* 13: 1711–1718.

Syrtzova, L. A., G. I. Likhtenshtein, I. I. Nazarova, T. N. Pisarkaya, and V. V. Nazarov. 1972. Study on the ATP-ase active center of nitrogenase by NMR method. *Dokl. Akad. Nauk SSSR.* 206:367–370 (in Russian).

Syrtzova, L. A., G. I. Likhtenshtein, T. N. Pisarkaya, V. L. Berdinskii, V. P. Lezina, and A. U. Stepanyants. l974. Estimation of the distance between the ATPase and substrate-binding sites in nitrogenase by the NMR-^{l}H method. *Mol. Biol.* 8:656–662.

Taborsky, G. 1979. Interaction of cytochrome c, ferrous ion, and phosphate. *Biochemistry.* 254:5246–5251.

Taylor, J. S., J. S. Leigh, and M. Cohn. 1969. Magnetic resonance studies of spin-labeled creatine kinase system and interaction of two paramagnetic probes. *Proc. Natl. Acad. Sci. USA.* 64:219–226.

Tidor, B., and M. Karplus. 1991. Simulation analysis of the stability mutant R96H of T4 lysozyme. *Biochemistry.* 30:3217–3228.

Tsui, F. C., S. A. Sundberg, and W. L. Hubbell. 1990. Distribution of charge on photoreceptor disk membranes, and implications for charged lipid asymmetry. *Biophys. J.* 57:85–97.

Vogel, V. R., E. T. Rubtsova, A. I. Kotelnikov, and G. I. Likhtenshtein. 1986. Investigation of protein diffusion collisions by method of triplet labels. *Biofizika.* 31:152–153.

Vold, R. L., J. S. Waugh, M. P. Klein, and D. E. Phelps. 1968. Measurement of spin relaxation in complex systems. *J. Chem. Phys.* 48: 3831–3836.

Wien, R. W., J. D. Morriset, and H. M. McConnell. 1972. Spin-label induced nuclear relaxation. Distances between bound saccharides, histidine-15, and tryptophan-123 on lysozyme in solution. *Biochemistry.* 11:3707–3716.

Yang, A.-S., M. R. Gunner, R. Sampogna, K. Sharp, and B. Honig. 1993. On the calculation of pK_as in proteins. *Proteins.* 15:252–265.